Available online at www.sciencedirect.com
SCIENCE DIRECT®
Composites Science and Technology 65 (2005) 37–46
COMPOSITES SCIENCE AND TECHNOLOGY
www.elsevier.com/locate/compscitech

Electrical resistance change method for monitoring delaminations of CFRP laminates: effect of spacing between electrodes

Akira Todoroki *, Miho Tanaka, Yoshinobu Shimamura

Department of Mechanical Sciences and Engineering, Tokyo Institute of Technology, 2-12-1 O-okayama, Meguro, Tokyo 1528552, Japan

Received 12 May 2003; received in revised form 17 May 2004; accepted 30 May 2004
Available online 31 July 2004

Abstract

The present study employs an electrical resistance change method for monitoring delamination. The authors have found that the electrical resistance change method using response surfaces is very effective in identify delaminations in CFRP laminates both experimentally and analytically. In the present study, the effect of the spacing between electrodes on the method is investigated using FEM analyses. Five types of spacing are analyzed here, and the two types of fiber volume fractions are also calculated. Cross-ply beam type specimens are adopted for the analyses. As a result, it was revealed that the effect of the spacing depends on the fiber volume fraction. For laminates of high fiber volume fraction, a short spacing is required to obtain high estimation performances of delamination location and length.

Keywords: A. Polymer–matrix composites; A. Smart materials; C. Delamination

1. Introduction

The electrical resistance change method uses multiple electrodes mounted on a target CFRP (carbon fiber reinforced plastics) laminate to measure electrical resistance changes. Electrical resistance changes between equally-spaced electrodes are measured with electrical resistance bridge circuits. The response surfaces are adopted to identify the locations and sizes of delaminations from these measured electrical resistance changes. After making these response surfaces, in this method, a delamination of a CFRP laminate is monitored by measuring electrical resistance changes.

The authors have published papers that adopt the electrical resistance change method [1–5]. This method has been found to be both experimentally and analytically efficient for the identification of a delamination in a CFRP laminated plate. Since the method adopts reinforcement carbon fibers as sensors for damage identification, this method does not cause a reduction in the static strength or fatigue strength; it is applicable to existing structures merely by the attachment of multiple electrodes. The electrical resistance change method, therefore, has been employed by many researchers for identifying internal damage such as fiber breakages and debonding between fibers and the matrix in CFRP laminates [6–13].

To improve the estimation performance of the delamination location with the electrical resistance change method, the authors have proposed a new method with normalizations of the electrical resistance change data [14]. The measured electrical resistance changes were normalized, and the response surfaces to estimate the locations and lengths of delaminations were made from the normalized electrical resistance changes and the norm. The new method has been applied to estimate the location of delaminations for beam-type specimens

* Corresponding author. Tel./fax: +81-3-5734-3178.
E-mail address: atodorok@ginza.mes.titech.ac.jp (A. Todoroki).

0266-3538/$ - see front matter © 2004 Elsevier Ltd. All rights reserved.
doi:10.1016/j.compscitech.2004.05.018

and the estimation performance was found to be significantly improved.

In our previous studies [1–5,14], multiple electrodes spaced regularly were mounted on a single specimen surface for both the analyses and the experiments. The spacing between the electrodes was set at 35 or 45 mm. In the present study, therefore, the effect of the spacing between electrodes is investigated analytically using FEM analyses. Using thin CFRP laminates, a large number of FEM analyses are performed using various spacings between electrodes. Our previous study [3] has shown that the electrical conductivity in the thickness direction and the transverse direction depends significantly on the fiber volume fraction. In the present study, therefore, two kinds of fiber volume fractions are adopted for investigating the effect of the electrical conductivity. Cross-ply thin CFRP laminates are employed here for FEM analyses. The estimation performances are compared with each other, and the width of the error band of the estimations of delamination length is obtained. Considering practical experimental work of the compression strength after low velocity impact, the optimal spacing between electrodes is decided for each case of fiber volume fractions.

2. Electrical resistance change method for delamination monitoring

Carbon fiber has a high electrical conductivity; the epoxy matrix is its insulator. The actual carbon fiber in a unidirectional ply is not straight. The curved carbon fibers contact one another, comprising a carbon-fiber network within a ply. The contact-network brings non-zero electric conductivity, even in the transverse direction. In the same way, the fiber-network produces non-zero electrical conductivity in the thickness direction in a ply. Electric conductivity in the transverse direction is much lower than that in the fiber direction. The authors [4] and Abry et al. [11] have found experimentally that the electrical conductivity ratio of the transverse direction (σ_{90}) to the fiber direction (σ_0) is very small, and that the electrical conductivity ratio of the thickness direction (σ_t) to the fiber direction is smaller than that of the transverse direction. The examples of the fiber volume fractions of 62% and 47% are shown in Table 1. The results indicate that CFRP laminates have significantly strong orthotropic electrical conductivity, and a small fiber volume fraction results in a small electrical conductivity. The electrical conductivity in the thickness direction and the transverse direction decreases significantly with a slight decrease in the fiber volume fraction from 62% to 47%.

Table 1
Measured electric conductivity of CFRP (after [4])

V_f	σ_0 (S/m)	σ_{90}/σ_0	σ_t/σ_0
0.47	4600	1.1×10^{-3}	2.2×10^{-4}
0.62	5500	3.7×10^{-2}	3.8×10^{-3}

Although the fiber-network structure in the thickness direction is almost identical to the structure of the transverse direction in a ply, the through-the-thickness conductivity σ_t is smaller than σ_{90} for normal laminates. That is because thin electrically insulating resin-rich interlamina exists there. For actual CFRP composites, however, prepreg plies are serpentine as the fibers in a ply. The ply curvature induces fiber contact through plies and causes non-zero electrical conductivity in the thickness direction, even for thick laminated CFRP laminates. Contact among plies causes non-zero electrical conductivity in the thickness direction. Thus, the σ_{90} is usually larger than the σ_t. When a crack grows in the interlamina, the crack breaks the fiber-contact-network between plies. A breakage of the contact network causes an increased electrical resistance in the CFRP composites.

Fig. 1 shows a schematic representation of the delamination-monitoring system proposed by the authors. Equally spaced multiple electrodes are mounted on the specimen surface, as shown in Fig. 1. All of these electrodes are placed on a single side of the specimen. Usually, it is impossible to place electrodes and lead wires outside of aircraft structures. The location of electrodes on the single surface is a model of the placement of electrodes inside a thin-shelled aircraft structure. The authors have performed several FEM analyses and concluded that the electrical current should be applied in the fiber direction of the surface ply for monitoring a delamination crack [4]. The electrical resistance change of each segment between electrodes is measured with a conventional electrical resistance bridge circuit. The electrical resistance changes among all segments are measured for various delamination sizes and locations. Using the measured data, the relationships between electrical resistance changes and delaminations (location and length of delaminations) are obtained using the response surfaces. The response surface method is similar to artificial neural networks. Usually, quadratic polynomials are adopted to obtain the relationship between the delamination location and electrical resistance changes or the relationship between delamination length and electrical resistance changes. The response surfaces of quadratic polynomials are employed here since the authors have revealed that the response surfaces are better than artificial neural networks for this inverse problem [2]. After calculations of the response surfaces, the delamination location and length can be estimated with the obtained response surfaces. The measured electrical resistance changes are substituted into the response surfaces and the estimated delamination location and length are obtained from the quadratic polynomials.

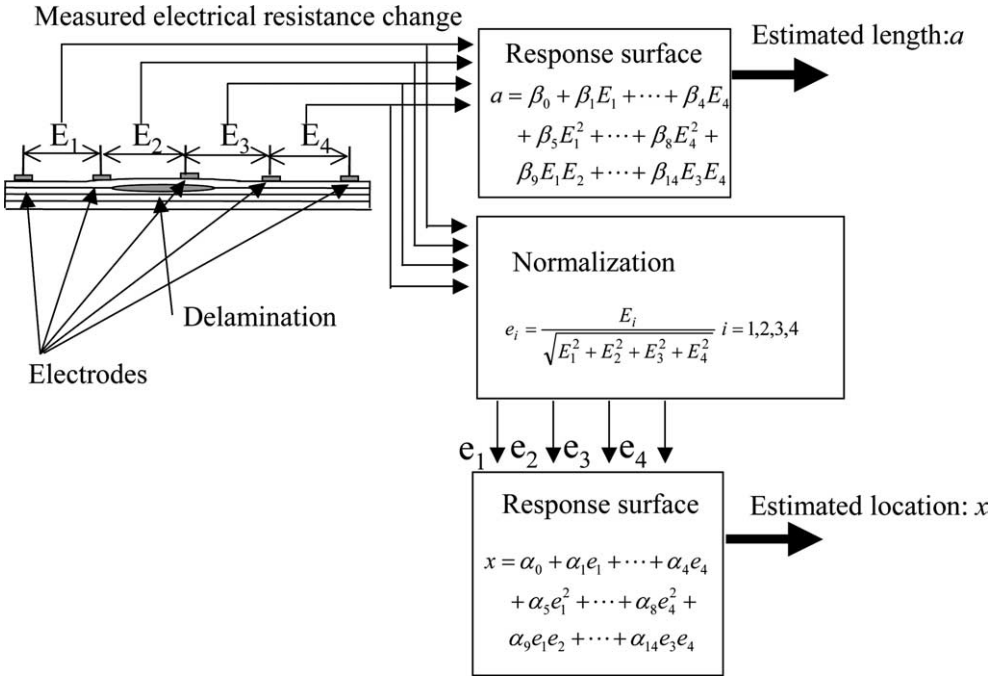

Fig. 1. Schematic representation of normalized electrical resistance change method.

In the case shown in Fig. 1, four electrical resistance changes are measured at four segments (obtained electrical resistance change: E_1, E_2, E_3 and E_4). Many experiments or calculations must be performed to make response surfaces for estimations of delamination location and length. Many data sets of delamination location, length and electrical resistance changes are obtained from experiments or FEM analyses. In the case of quadratic polynomials, the response surfaces estimating the delamination length (a) are as follows:

$$\begin{aligned} a = {} & \beta_0^a + \beta_1^a E_1 + \beta_2^a E_2 + \beta_3^a E_3 + \beta_4^a E_4 + \beta_5^a E_1^2 + \beta_6^a E_2^2 \\ & + \beta_7^a E_3^2 + \beta_8^a E_4^2 + \beta_9^a E_1 E_2 + \beta_{10}^a E_1 E_3 + \beta_{11}^a E_1 E_4 \\ & + \beta_{12}^a E_2 E_3 + \beta_{13}^a E_2 E_4 + \beta_{14}^a E_3 E_4, \end{aligned} \tag{1}$$

where all of the coefficients (β_i^a, $i = 1, \ldots, 14$) are obtained with the least square errors method [15]. For example, at least 14 sets of electrical resistance changes of various delamination locations and sizes are required. Usually, the number of data points in 14 sets is too small, and two times the number of unknown coefficients is required.

To improve the estimation performance of the delamination location, the normalizations of the measured electrical resistance change are performed. In the case of four segments, each measured result is normalized by means of the norm of the vector of measured electrical resistances. Each element is divided by the square root sum of all four results as follows:

Before normalization: (E_1, E_2, E_3, E_4)

After normalization:

$$(e_1, e_2, e_3, e_4) = \left(\frac{E_1}{\sqrt{E_1^2 + E_2^2 + E_3^2 + E_4^2}}, \frac{E_2}{\sqrt{E_1^2 + E_2^2 + E_3^2 + E_4^2}}, \frac{E_3}{\sqrt{E_1^2 + E_2^2 + E_3^2 + E_4^2}}, \frac{E_4}{\sqrt{E_1^2 + E_2^2 + E_3^2 + E_4^2}} \right). \tag{2}$$

Using these normalization results, a response surface for estimating the delamination locations (x) is made as follows:

$$\begin{aligned} x = {} & \beta_0^x + \beta_1^x e_1 + \beta_2^x e_2 + \beta_3^x e_3 + \beta_4^x e_4 + \beta_5^x e_1^2 + \beta_6^x e_2^2 \\ & + \beta_7^x e_3^2 + \beta_8^x e_4^2 + \beta_9^x e_1 e_2 + \beta_{10}^x e_1 e_3 + \beta_{11}^x e_1 e_4 \\ & + \beta_{12}^x e_2 e_3 + \beta_{13}^x e_2 e_4 + \beta_{14}^x e_3 e_4, \end{aligned} \tag{3}$$

where all coefficients (β_i^x, $i = 1, \ldots, 14$) are obtained with the least square errors method as well [15]. The lack of fit is evaluated with the adjusted coefficient of the multiple determination R_{adj}^2 [15]; R_{adj}^2 is defined as

$$R_{\text{adj}}^2 = 1 - \frac{SS_{\text{E}}/(n-k-1)}{S_{yy}/(n-1)}, \tag{4}$$

where SS_{E} is the square sum of errors, S_{yy} is the total sum of squares, n is the number of data sets, and k is the number of unknown coefficients. The value of R_{adj}^2 is equal to or lower than 1.0. A higher value of R_{adj}^2 implies a better fit. When the response surface shows a very good fit, R_{adj}^2 approaches 1.0. A good fit of the response surface means that the response surface gives good estimations for the electrical resistance changes used for the

regression. Lower R^2_{adj} values means poorer estimations and the error band of the estimated result is wider.

In our previous study, the response surfaces obtained from the experimental data provided excellent estimations of the delamination locations of beam-type specimens [3] and plate-type specimens [5]. FEM analyses gave similar results to the experimental results [1,2,4]. Since FEM is convenient for parameter analyses, FEM analyses are employed here.

Since all of the coefficients can be obtained from the least square errors method, a lot of experiments or FEM calculations must be performed to obtain a sufficient number of sets of electrical resistance changes. This is the main drawback of the method identified so far.

3. FEM analysis

In the present study, FEM analyses are employed for investigations. Beam-type specimens were adopted for FEM analyses of delamination monitoring, as shown in Fig. 2. The specimen has seven equally spaced electrodes on the surface. Five types of spacing between electrodes are adopted here: 15, 30, 45, 60 and 75 mm. Since the spacing is different for each type of specimen, the beam length is different in each specimen. The total length of the beam (L) can be calculated with spacing (S) as $L = 10 + 10 + 6 \times S$ (mm): each outermost electrode has a fringe of 10 mm in length. The beam thickness is 2 mm. The stacking sequence of the specimen is [0/90] s. In this study, each ply thickness is fixed at 0.5 mm, four times larger than the normal prepreg.

Since the diameter of a typical carbon fiber is much smaller than the size of the FEM elements adopted here, the inhomogeneous orthotropic CFRP composite material is assumed to be a homogeneous orthotropic material for the present FEM analyses. In the thickness direction, however, the thickness of the resin-rich layer, which causes lower electrical conductivity compared to that of the transverse direction, is smaller than the ply thickness. This introduces the difficulty of modeling electrical conductivity in the thickness direction. In the present study, four-node-rectangular elements are adopted for the analysis; each element is approximately 0.0625 mm × 0.25 mm. Since the ply thickness is 0.5 mm, a ply comprises eight elements in the thickness direction. This implies that the average electrical conductivity in the thickness direction in a ply can be obtained by assuming a homogeneous electrical conductivity in the thickness direction. Therefore, the electrical conductivity in the thickness direction is treated here as being approximately homogeneous.

The FEM analyses are performed using a commercially available FEM tool named ANSYS. A delamination crack is usually made at the interlayer between 0° ply and 90° ply; it is located opposite the impacted surface. To simulate this delamination location, a delamination crack should be made at the interface near the inside surface. In this study, the outside surface is the bottom surface and the inside surface is the top surface, as in Fig. 2. Therefore, a delamination crack is made at the interface between the top 0° ply and the middle 90° ply, as shown in Fig. 2. On the delamination crack surface lines, all nodes are doubly defined to represent the delamination crack surfaces. When a delamination crack is created, the doubly defined nodes on the delamination crack surfaces are released with each other to represent the electrical current insulation. For a delamination crack induced in the FEM model, the present study assumes that the crack mouth is fully opened after delamination, although an actual delamination crack has a crack surface contact. This may cause an overestimation in the electrical resistance changes. However, our previous studies have shown that the FEM results provide not only very good qualitative analyses but also similar electrical resistance changes [1–5].

Table 1 shows the electrical conductivity used for the FEM analysis. To compute the electrical resistance changes, a direct electric current of 30 mA is charged from one electrode; also, the electrical voltage of the other side of the segment is set to 0 V. After computation, the electrical voltage at the electrode is divided by the electrical current (30 mA) to calculate the electrical resistance of the segment. After this computation, a delamination is created and a similar computation is conducted to obtain the electrical resistance changes at the segment. In the present study, since the total number of electrodes is seven, the total number of segments is six.

Definitions of the delamination length and location are also shown in Fig. 2. The delamination location is

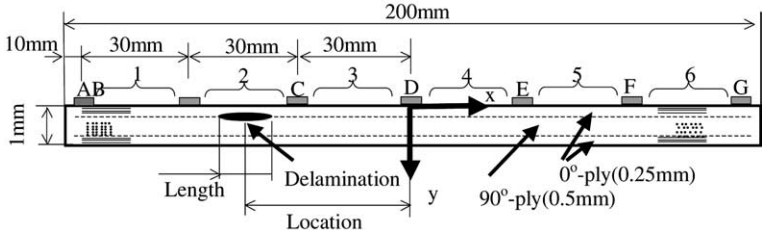

Fig. 2. Specimen configuration of beam for FEM analyses (spacing $S = 30$ mm.)

defined as the location of the center of the delamination crack from the middle of the specimen. The delamination location in the thickness direction is ignored in the present study because the laminate is thin.

Various types of delaminations are computed to obtain the electrical resistance changes. The total number of analyses is 165 for each specimen. Five types of length of delamination are computed: 5, 10, 20, 30 and 40 mm.

4. Results and discussion

4.1. Estimations of delamination location

Fig. 3 shows the estimated results of the delamination location for the case in which the fiber volume fraction is $V_f = 0.472$ and the spacing between electrodes is $S = 30$mm. In this figure, the abscissa is the given delamination location and the ordinate is the estimated delamination location with the response surface made from the normalized electrical resistance changes. Almost all of the points are located on the diagonal line, showing that the estimations are very exact. The R^2_{adj} of this result is 0.996. Most of the estimations are plotted on the diagonal line. The width of the error band is defined to be the maximum error in the calculated results in the present study. The error band from the diagonal line is very narrow, as shown in Fig. 3.

Fig. 4 shows the estimated results of the delamination location for the case where the fiber volume fraction is $V_f = 0.621$ and the spacing between electrodes is $S = 30$ mm. The abscissa and the ordinate are the same as those in Fig. 3. The R^2_{adj} of this result is 0.987, and the value is smaller than that of Fig. 3. The smaller value of R^2_{adj} means a wider error band. Thus, the value of R^2_{adj} refers to the fit of the curve and the relative change in the width of the error band.

Fig. 5 shows the results of R^2_{adj} for all cases of both fiber volume fractions. The solid circles represent the cases for $V_f = 0.472$ and the open circles represent the cases for $V_f = 0.621$. The abscissa is the spacing between electrodes and the ordinate is the value of R^2_{adj}.

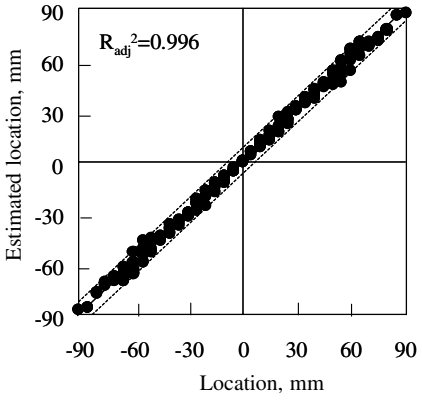

Fig. 3. Estimated location in case of $V_f = 0.472$ and spacing between electrode $S = 30$ mm.

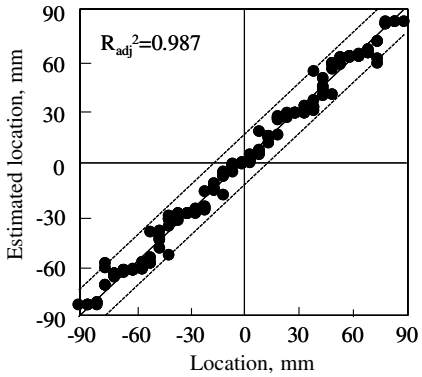

Fig. 4. Estimated location in case of $V_f = 0.621$ and spacing between electrodes $S = 30$ mm.

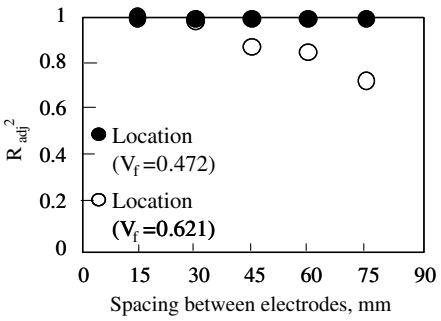

Fig. 5. Results of estimated location due to spacing between electrodes.

For the case where $V_f = 0.472$, the values of R^2_{adj} are constant at almost 1.0. This means that the error band width does not increase with increasing spacing between electrodes. On the other hand, for the case where $V_f = 0.621$, the values of R^2_{adj} decrease with increasing spacing between electrodes. This means that the error band width increases with increasing spacing between electrodes. Let us check the estimation results of the worst case of $V_f = 0.621$ and $S = 75$ mm. Fig. 6 shows the results of the estimations. In this figure, the estimations of the smallest delaminations of length 5 mm are represented as solid circle symbols, and the other delaminations are shown as open circle symbols. As shown in this figure, only the delaminations that are located at the middle of the segment between electrodes show very poor estimations. The results of FEM analyses of these short delaminations at the middle of the segments give no electrical resistance changes whatsoever. The no electrical resistance changes of short delaminations at the middle of the segments result in large estimation errors.

If we adopt artificial neural networks instead of using the response surfaces, we can surely reduce the error band for most of the cases by means of a long training

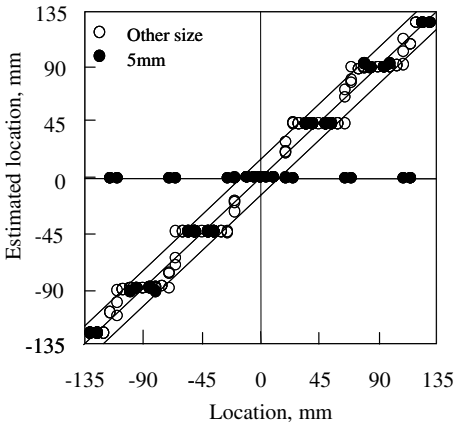

Fig. 6. Estimated location in case of $V_f = 0.621$ and spacing between electrodes $S = 45$ mm.

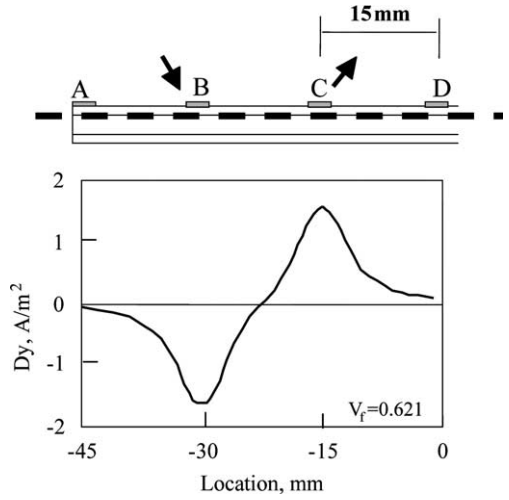

Fig. 7. Electric current density distribution in case of $V_f = 0.621$ and spacing between electrode $S = 15$ mm.

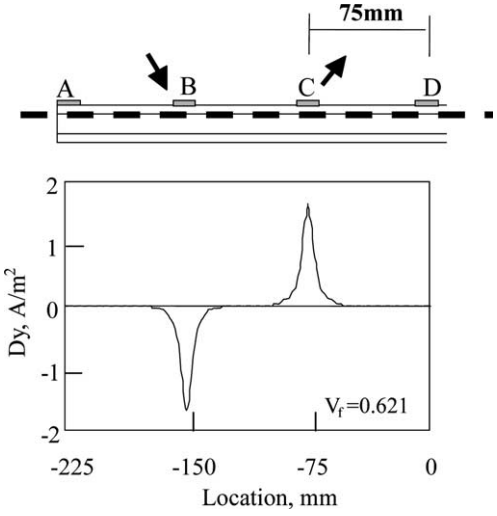

Fig. 8. Electric current density distribution in case of $V_f = 0.621$ and spacing between electrode $S = 75$ mm.

time of the artificial neural networks. Our previous study [2], however, revealed that fully trained neural networks provide poor estimations for new data sets that are not used for the training of neural networks. This is similar to the well-known fact that a higher order polynomial can be fit to a higher nonlinear relationship but may give poor estimations for new data that are not used for the regression. Since the performance of estimations for the new data cannot be obtained perfectly without calculations of the entire possible cases, we employ quadratic polynomials as basic functions of the response surfaces as in our previous paper [2] to reduce the risk of poor estimations for the new data. Moreover, the previous study reveals that the estimation error of the new data for the quadratic polynomials is almost within the same variant as the width of the estimation error to the regressed sets of data. In the present study, therefore, only regressed sets of data are dealt with, without mentioning the new data.

To investigate the reason for the disappearance of electrical resistance changes for small delaminations at the middle of the segment, the electrical current density of four typical specimens are plotted as shown in Figs. 7–10. In these figures, the abscissa is the location of the longitudinal axis of the beam-type specimen: The origin of the location is the middle of the beam specimens. The ordinate is the electrical current density of the thickness direction at the interface between 0° ply and 90° ply where a delamination is created.

Fig. 7 shows the results of the case of $V_f = 0.621$ and a spacing between electrodes of $S = 15$ mm. Fig. 8 shows the results of the case of $V_f = 0.621$ and a spacing between electrodes of $S = 75$ mm. In both cases, the electric current density in the thickness direction is large under electrodes B and C where the electrical current is applied. For the short spacing case (see Fig. 7), however, the electric current density in the thickness direction exists in the entire region, not only in the segment where the electrical current is applied but also in adjacent segments. For the long-spacing case (see Fig. 8), in contrast, the electrical current density in the thickness direction does not exist at the middle of the segment where the electrical current is applied. Fig. 9 shows the results of the case of $V_f = 0.472$ and a spacing between electrodes of $S = 15$ mm. Fig. 10 shows the results of the case of $V_f = 0.472$ and a spacing between electrodes of $S = 75$ mm. In these cases, even for the long spacing case (see Fig. 10), the electrical current density in the thickness direction exists in the entire region in the segment where the electrical current is applied. The lack of electrical current at the middle of the segment causes there to be no electrical resistance changes for small delaminations for the case of $V_f = 0.621$ and a spacing between electrodes of $S = 75$ mm.

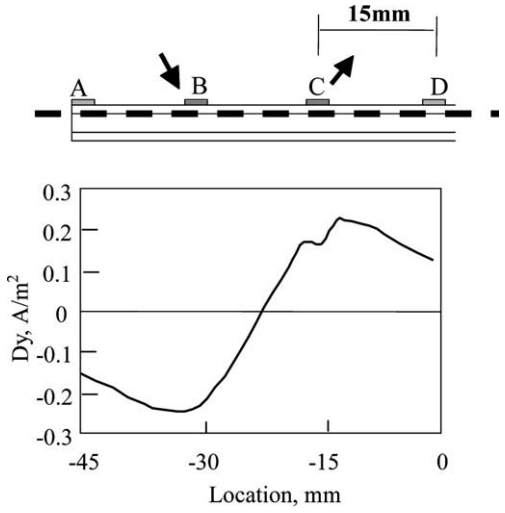

Fig. 9. Electric current density distribution in case of $V_f = 0.472$ and spacing between electrode $S = 15$ mm.

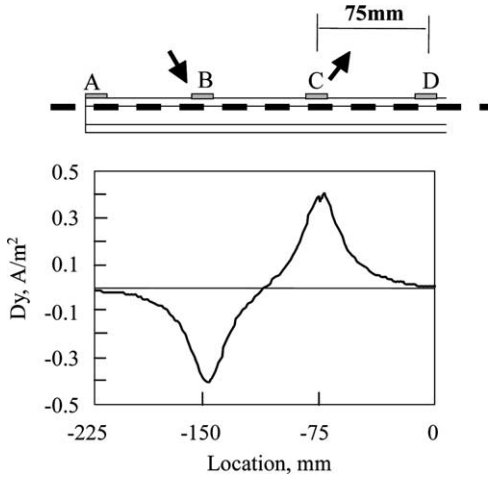

Fig. 10. Electric current density distribution in case of $V_f = 0.472$ and spacing between electrode $S = 75$ mm.

4.2. Estimation of delamination length

The results of R^2_{adj} of the response surfaces for the estimations of the delamination length are shown in Fig. 11. The abscissa is the spacing between electrodes and the ordinate is the calculated R^2_{adj}. For the cases of $V_f = 0.472$, the values of R^2_{adj} are kept at a high value, even for the large spacing ($S = 75$ mm). For the cases of $V_f = 0.621$, however, the values of R^2_{adj} decrease rapidly with increasing spacing.

Fig. 12 shows the estimated results of the delamination length for the case where the fiber volume fraction is $V_f = 0.472$ and the spacing between electrodes is $S = 15$ mm. In this figure, the abscissa is the given delamination length and the ordinate is the estimated delamination length with the response surface made from the electrical resistance changes. The plots on the diagonal line mean that the estimations are very exact. The

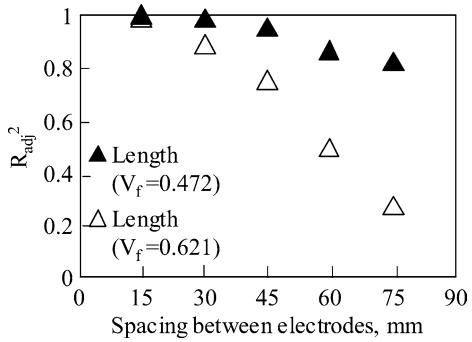

Fig. 11. Results of the estimated length due to spacing between electrodes.

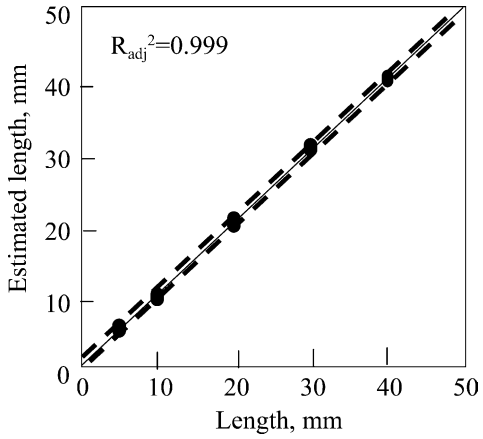

Fig. 12. Estimated length in case of $V_f = 0.472$ and spacing between electrodes $S = 15$ mm (error band 1 mm).

R^2_{adj} is 0.999 in this case. All of the estimations are plotted on the diagonal line. The error band is defined as the maximum error of the estimated length from the given one in the calculated results here. The error band from the diagonal line is less than 1 mm, as shown in Fig. 12.

Fig. 13 shows the estimated results of delamination length for the case where the fiber volume fraction is $V_f = 0.472$ and the spacing between electrodes is $S = 45$ mm. The R^2_{adj} of this result is 0.9575. Most of the estimations are plotted around the diagonal line, but the error band of the estimations is 10 m and the value is wider than that of Fig. 12. Fig. 14 shows the estimated results of the delamination length for the case where the fiber volume fraction is $V_f = 0.472$ and the spacing between electrodes is $S = 75$ mm. The R^2_{adj} of this result is 0.820. Although most of the estimations are plotted around the diagonal line, the error band of the estimations is 17 mm. These figures show that the increase in spacing causes an increase in the error band for the estimations of the delamination length, even for the laminates for which $V_f = 0.472$.

Fig. 15 shows the estimated results of the delamination length for the case where the fiber volume fraction is $V_f = 0.621$ and the spacing between electrodes is $S = 15$ mm. The R^2_{adj} of this result is 0.989. Most of

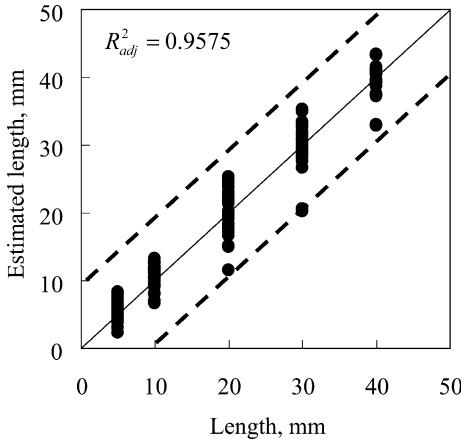

Fig. 13. Estimated length in case of $V_f = 0.472$ and spacing between electrodes $S = 45$ mm (error band 10 mm).

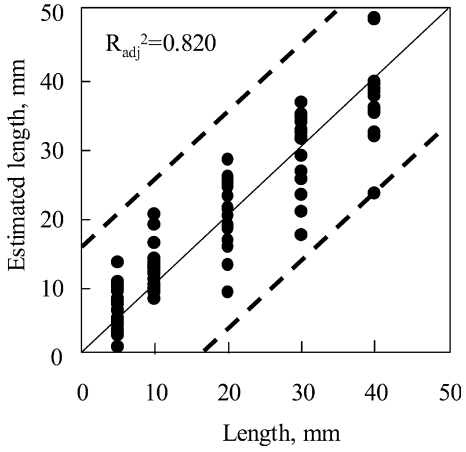

Fig. 14. Estimated length in case of $V_f = 0.472$ and spacing between electrodes $S = 75$ mm (error band 17 mm).

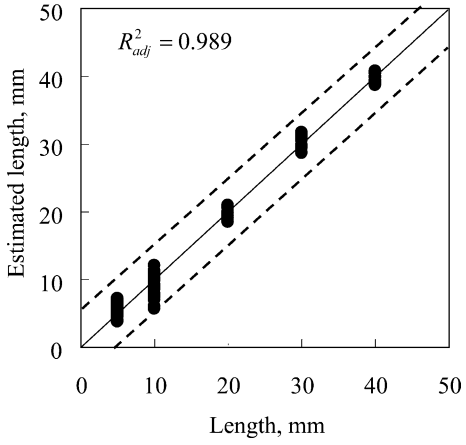

Fig. 15. Estimated length in case of $V_f = 0.621$ and spacing between electrodes $S = 15$ mm (error band 5 mm).

the estimations are plotted around the diagonal line. The error band is only 5 mm, as shown in Fig. 15. Fig. 16 shows the estimated results of the delamination length for the case where the fiber volume fraction is $V_f = 0.621$ and the spacing between electrodes is $S = 45$ mm. The R^2_{adj} of this result is 0.752. Most of the estimations are scattered, and the error band is 20 mm. Fig. 17 shows the estimated results of the delamination length for the case where the fiber volume fraction is $V_f = 0.621$ and the spacing between electrodes is $S = 75$ mm. The R^2_{adj} of this result is 0.270. Most of the estimations are highly scattered and the error band is 22 mm. Although the width of the error band is only 2 mm wider than the case for which $S = 45$ mm, the estimation performance seems awful, and the response surface is essentially useless for the estimation of delamination length.

Fig. 18 shows the results of the error bands for various spacings. The abscissa is the given spacing and the ordinate is the calculated width of the error band. As shown in this figure, the width of the error band

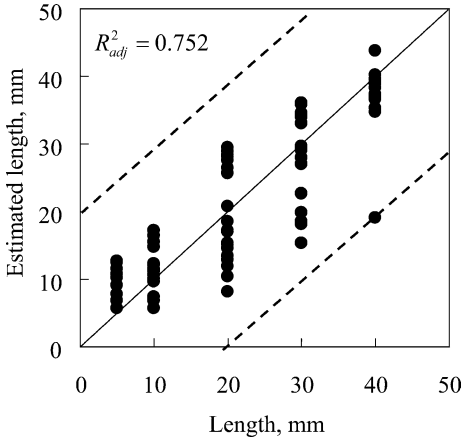

Fig. 16. Estimated length in case of $V_f = 0.621$ and spacing between electrodes $S = 45$ mm (error band 20 mm).

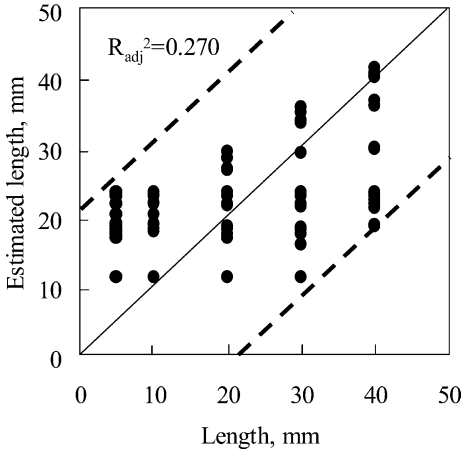

Fig. 17. Estimated length in case of $V_f = 0.621$ and spacing between electrodes $S = 75$ mm (error band 22 mm).

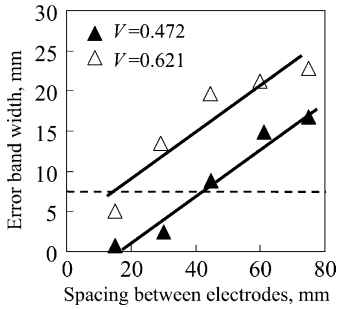

Fig. 18. Results of the estimated error band due to spacing between electrodes.

increases approximately linearly with increasing spacing, and the slopes of both of the fiber volume fractions are almost the same.

Crantwell and others have shown that the low velocity impact induced a delamination in a CFRP plate [16]. They showed that a delamination of 50 mm^2 might cause a reduction in the compression strength of approximately 20%. Of course, although the size of the delamination depends on the stacking sequence and materials of the CFRP laminates, the maximum allowable error can be estimated using this result. If we consider a simple rectangular delamination for a beam-type specimen, the allowable length is approximately 7 mm ($50 \approx 7 \times 7$). The line of error of 7 mm is shown in Fig. 18 as a dashed horizontal line.

For larger spacings we do not have to prepare many electrodes on the target CFRP laminate. Therefore, the larger spacing is better for actual delamination monitoring. The larger spacing, however, gives poor estimations, as shown in Fig. 18. The cross-points between the dashed line and the line of the error band shows that the appropriate spacing is 15 mm for laminates of $V_f = 0.621$, and similarly the appropriate spacing is 45 mm for laminates of $V_f = 0.472$. The appropriate spacing depends on the fiber volume fraction. A larger fiber volume fraction requires a shorter spacing to obtain a sufficient performance in the estimations. That is because the electrical current density in the thickness direction depends on the fiber volume fraction, as discussed in the previous section.

5. Conclusions

The present study deals with the effect of the spacing between electrodes for the electrical resistance change method to identify the delamination locations and lengths of beam-type specimens. FEM analyses are employed to investigate the effect here. Cross-ply laminates of CFRP are adopted, and the response surfaces are used to solve the inverse problems. Two types of fiber volume fractions are investigated. The results obtained are as follows:

(1) For the laminates of $V_f = 0.472$, the estimation performance of the delamination location does not decrease, even for large spacings of 75 mm.
(2) For the laminate of $V_f = 0.621$, the estimation performance of the delamination location decreases with increasing spacing between electrodes. This decrease is caused by the poor estimations of the small delaminations that are located at the middle of the segment between electrodes.
(3) For both laminates, the estimation performance of the delamination length decreases with increasing spacing. For the laminates of $V_f = 0.621$, the performance significantly decreases compared with the results of $V_f = 0.472$.
(4) The allowable error for the delamination length estimations depends on the fiber volume fractions. For the laminates of large fiber volume fractions, a smaller spacing between electrodes is required to maintain a high estimation performance for identifications.

References

[1] Todoroki A, Suzuki H. Health monitoring of internal delamination cracks for graphite/epoxy by electric potential method. Appl Mech Eng 2000;5(1):283–94.
[2] Todoroki A. Effect of number of electrodes and diagnostic tool for delamination monitoring of graphite/epoxy laminates using electric resistance change. Compos Sci Technol 2001; 61(13):1871–80.
[3] Todoroki A, Tanaka Y. Delamination identification of cross-ply graphite/epoxy composite beams using electric resistance change method. Compos Sci Technol 2002;62(5):629–39.
[4] Todoroki A, Tanaka M, Shimamura Y. Measurement of orthotropic electric conductance of CFRP laminates and analysis of the effect on delamination monitoring with electric resistance change method. Compos Sci Technol 2002;62(5):619–28.
[5] Todoroki A, Tanaka Y, Shimamura Y. Delamination monitoring of graphite/epoxy laminated composite plate of electric resistance change method. Compos Sci Technol 2002;62(9):1151–60.
[6] Schulte K, Baron Ch. Load and failure analyses of CFRP laminates by means of electrical resistively measurements. Compos Sci Technol 1989;36(1):63–76.
[7] Muto N, Yanagida H, Miyayama M, Nakatsuji T, Sugita M, Ohtsuka Y. Foreseeing of fracture in CFGFRP composites by measuring electric resistance. J Jpn Soc Compos Mater 1992;18(4):144–50 [in Japanese].
[8] Chen PW, Chung DDL. Carbon fiber reinforced concrete for smart structures capable of non-destructive flaw detection. Smart Mater Struct 1993;2(1):22–30.
[9] Kaddoour AS, Al-Salehi FA, Al-Hassani STS. Electrical resistance measurement technique for detecting failure in CFRP materials at high strain rate. Compos Sci Technol 1994;51(3):377–85.
[10] Irving PE, Thiagarajan C. Fatigue damage characterization in carbon fibre composite materials using an electric potential technique. Smart Mater Struct 1998;7(4):456–66.
[11] Abry JC, Bochard S, Chateauminois A, Salvia M, Giraud G. In situ detection of damage in CFRP laminates by electric resistance measurements. Compos Sci Technol 1999;59(6):925–35.

[12] Seo DC, Lee JJ. Damage detection of CFRP laminates using electrical resistance measurement and neural network. Compos Struct 1999;47(1–4):525–30.
[13] Schueler R, Joshi SP, Schulte K. Damage detection in CFRP by electrical conductance mapping. Compos Sci Technol 2001;61(6):921–30.
[14] Todoroki A, Tanaka M, Shimamura Y. High performance estimations of delamination of graphite/epoxy laminates with electric resistance change method. Compos Sci Technol 2003;63(13):1911–20.
[15] Myers R, Montgomery DC. Response surface methodology process and product optimization using designed experiments. 2nd ed. New York: Wiley–Interscience; 2002.
[16] Crantwell WJ, Curtis P, Morton J. An assessment of the impact performance of CFRP reinforced with high-strain carbon fibres. Compos Sci Technol 1986;25(2):133–48.